TÜBİTAK

Turkish Journal of Earth Sciences

http://journals.tubitak.gov.tr/earth/

Research Article

Turkish J Earth Sci
(2015) 24: 39-55

doi:10.3906/yer-1410-7

Discovery of hiatus in Feixianguan Formation and its geological implications, Sichuan Basin, SW China

Yang YU[1,2], Xiucheng TAN[1,3,*], Peiyuan CHEN[1,2], Huiting YANG[2], Teng MA[1], Jian CAO[4], Xiuju JIN[5]

[1]State Key Laboratory of Oil and Gas Geology and Exploration, Southwest Petroleum University, Chengdu, P.R. China
[2]Provincial Key Laboratory of Natural Gas Geology, Southwest Petroleum University, Chengdu, P.R. China
[3]School of Earth Sciences and Technology, Branch of Sedimentology and Hydrocarbon Accumulation, CNPC Key Laboratory of Carbonate Reservoir, Southwest Petroleum University, Chengdu, P.R. China
[4]Department of Earth Sciences, Nanjing University, Nanjing, Jiangsu, P.R. China
[5]Research Institute of Petroleum Exploration and Development, Zhongyuan Oilfield, Puyang, P.R. China

Received: 06.10.2014 • **Accepted:** 03.11.2014 • **Published Online:** 02.01.2015 • **Printed:** 30.01.2015

Abstract: The lower Triassic Feixianguan Formation of the Sichuan Basin is an important exploration target for marine natural gas in China. It is widely believed that a certain interval from Fei 1 to Fei 4 displays conformable contacts rather than long-term wide-ranging hiatus. However, 2 denudational interfaces on the top of Member Fei 1 and Fei 2 respectively were found in the present work, which relies on the delicate core observation of 4 cored wells in Puguang Gas Field, microscopic observations of microsamples in terms of thin sections, scanning electron microscopy and cathodoluminescence, and geochemical testing. Evidence indicates that on the top of the first and second Member of Feixianguan Formation there existed karst unconformities, which is in distinguished contrast to previous interpretations of conformable contacts. According to those geological and geochemical investigations, a new classification is proposed for the interior Feixianguan Formation. The tectonic episode division of Indosinian movement consequently may be modified from the previous conception of a first-order episode to 3 sub-first-order episodes that correspond to the impact of 2 uplifting processes during the early Indosinian orogeny. These uplifting processes are the cause in interpreting the pervasive exposure and unconformable interfaces in Fei 1 and Fei 2 karstifications. Thus, we suggest another appropriate division of 3 third-order sequences that may suit the Feixianguan Formation, which correspond to Fei 1, Fei 2, and Fei 3–Fei 4. Regional reservoir formation was also largely affected by penecontemporaneous karstification. Massive dissolution pores fill with seepage sediments but generally remain effective reservoir spaces.

Key words: Hiatus, unconformity, penecontemporaneous karst, sequence interface, carbonate reservoir, Feixianguan Formation, Puguang Gas Field, Sichuan Basin

1. Introduction

The lower Triassic Feixianguan Formation of the Sichuan Basin is an important exploration target of marine-sourced natural gas in China, which was considered to exhibit conformable contacts from the bottom Member Fei 1 to the uppermost Member Fei 4 (No. 2 Sichuan Regional Geological Survey Team of the Sichuan Bureau of Geology, 1966, 1967). However, several scholars (Ma et al., 2005; Qiao et al., 2010; Shen et al., 2010; Guo, 2011) suggested that unconformities may occur in the Feixianguan Formation, especially between Member Fei 2 and Fei 3. If this is true, massive fundamental geological recognitions, including sedimentary cycle, sequence interface, and tectonic episode, have to be reconsidered for further Feixianguan reservoir exploration.

* Correspondence: tanxiucheng70@163.com

However, these points are still uncertain due to the shortage of sound evidence. Assisted by the Puguang Gas Field, the latest 4 cored-well observations and associated samplings are presented in this study, which provides credible material to address these issues. Based on the experimental data, we found some sound evidence for the existence of hiatus in the Feixianguan Formation between Member Fei 2 and Fei 3, and we identified another hiatus between Member Fei 1 and Fei 2. These findings provide new geological implications for the formation of the Feixianguan reservoir.

2. Geological setting

The Sichuan Basin is situated in the Yangtze paraplatform, SW China (Figure 1a). This depression, bordered by the

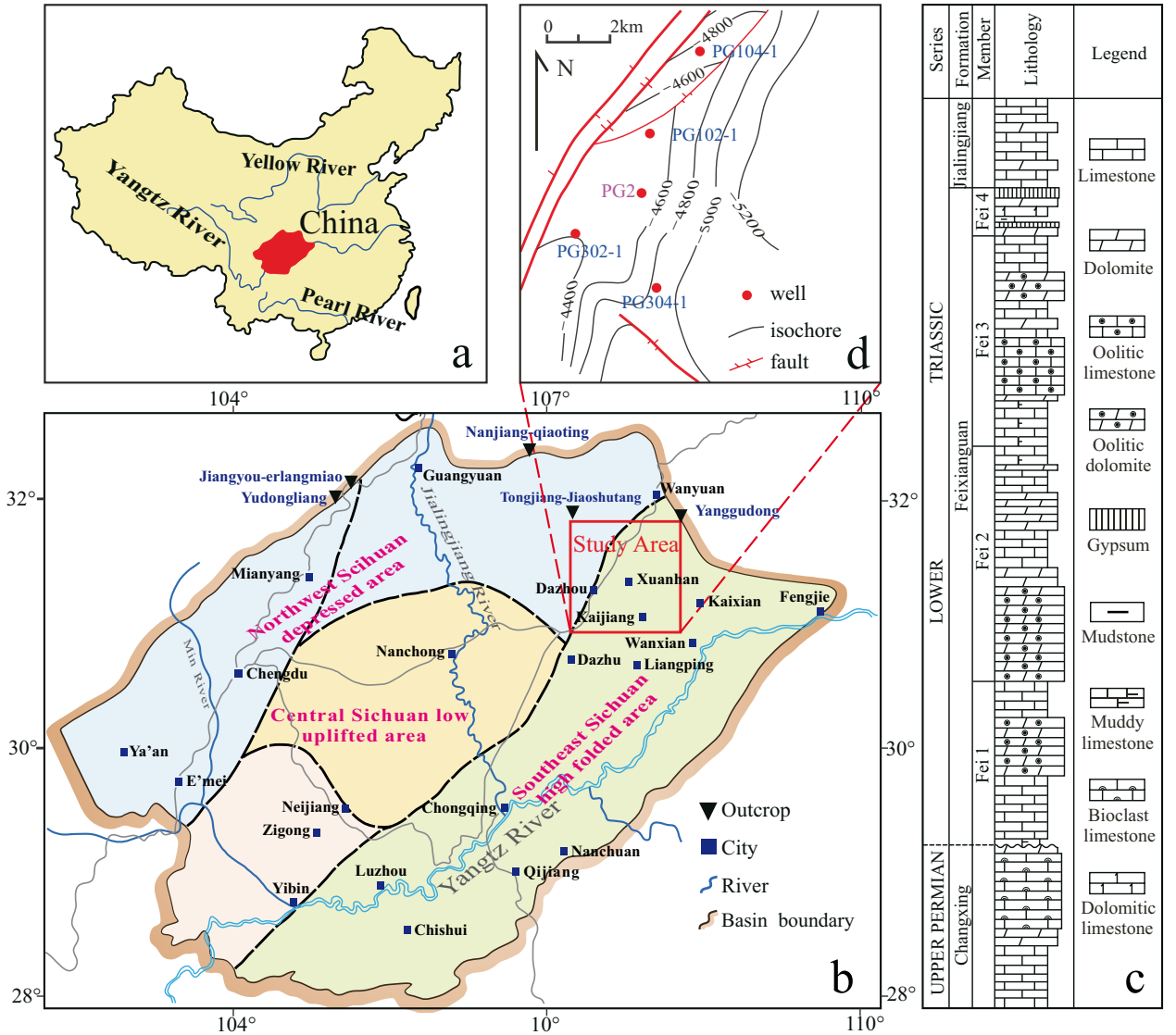

Figure 1. Regional tectonic setting of the study area and the stratigraphic column of the Feixianguan Formation.

Qinling fold zone to the north and the Songpan-Ganzi fold zone to the west, is a rhombus basin crossed by deep faults to the northeast and northwest (Sichuan Oil & Gas Field Geology Compilation Group, 1989). The peripheral tectonic units are tightly linked with the development of the Sichuan Basin, which can be divided from the west to the east into the northwest Sichuan depression zone, central Sichuan transitional uplift zone, and southeast Sichuan high fold belt (Wang ZC et al., 2002). The study area lies in the junction of the first and last units (Figure 1b), where the Puguang Gas Field (covering Xuanhan and Daxian county) is located.

The study area has largely experienced 5 tectonic cycles since the Ediacaran Period: the Caledonian, Hercynian, Indosinian, Yanshanian, and Himalayan (Ma et al., 2002), of which the former 3 span over the period of the Ediacaran-Triassic, characterized by inherited uplift and local rise and fall. During the latter 2 periods, the region suffered from intense intracontinental horizontal contraction, transmitting energy across the orogenic belt of Daba, Micang, and Wuling-Xuefeng, resulting in large-scale folds and thrust faults (Tang et al., 2008). No other tectonic movement is more active than that of the early Triassic Feixianguan (corresponding to the Indosinian) period in all Tethyan evolution history. The tectonic movement in the Feixianguan period dominated the essential platform and trough distribution pattern extending from the eastern to the western part of the Sichuan Basin (Guo et al., 2011). Northeastern Sichuan thus became a comparatively tranquil setting favoring platform deposition, while in the distant northwestern region volcanogenic sediments were formed (Qiao et al., 2010). Various studies indicate that

a surface of unconformity exists between the Feixianguan Formation and its underlying Changxing Formation of the Upper Permian, whereas the contact between the Feixianguan Formation and its overlying Jialingjiang Formation in the lower Triassic is conformable (Wei et al., 2004). According to the latest drilling data, the thickness of the Feixianguan Formation ranges from 350 to 700 m in the study area, which accordingly can be classified from the bottom to the top into 4 lithologic members: Fei 1, Fei 2, Fei 3, and Fei 4 (Figure 1c).

3. Materials and methods

This study is based on 4 cored wells (Figure 1d) (PG 102-1, PG 104-1, PG 302-1, and PG 304-1 wells; 'PG' stands for Puguang Gas Field), and the data were obtained using a combination of lithological and geochemical methods. A cumulative length of the 4 cored wells of 631 m was collected, which primarily consisted of only 3 members from the bottom to the top: Fei 1, Fei 2, and Fei 3. Thin-section analysis was performed for more than 1200 samples, of which 74 samples were selected for geochemical test analysis: 34 samples for carbon (C) and oxygen (O) isotopic analysis, 20 samples for strontium (Sr) isotopic analysis (from well PG 302-1), and 20 samples for major and trace elements analysis.

C and O isotopic analyses were performed in the geological laboratory of the Research Institute of Exploration and Development of the PetroChina Southwest Oil and Gas Field Company. Ground into powder, filtered through a 200-mesh sieve, and dried in an oven, the samples were subsequently preprocessed to react with 100% orthophosphoric acid for 24 h at 25 °C in a vacuum system. CO_2 values were obtained by measurement with a MAT-252 mass spectrometer, and the per-thousand differences in derived C and O isotope levels were standardized by PDB standard. The measurement accuracy was 0.1‰.

Sr isotopic analyses were performed in the General Resource Development and Environment Analysis and Testing Center of Guizhou Province. Samples (70 mg) were crushed until they passed through a 200-mesh sieve and were dissolved in a 0.8 N HCl solution in a Teflon cup for 2 h. After centrifugation, the supernatant was passed through an AG50 × 8 (H^+) cation exchange column, and the pure Sr was washed out using HCl as the eluent. The measurement was performed on a MAT262 solid isotope mass spectrometer. The blank background in the whole process was approximately 2×10^{-10} to 5×10^{-10} and error is expressed as 2σ (±).

The content analysis of typical elements and compounds, such as CaO, MgO, Mn, Fe, and Sr, was also performed in the General Resource Development and Environment Analysis and Testing Center of Guizhou Province. The CaO and MgO content was measured with conventional methods of chemical analysis with a detection threshold of 1% and errors of analysis of 2% and 5%, respectively. The Fe content was measured by a colorimetric method with a detection threshold of 0.01% and an error of less than 3%. The Mn and Sr contents were measured by atomic absorption spectrophotometry with detection thresholds of 5×10^{-6} and 42×10^{-6}, respectively, and errors of analysis of 13% and 14%, respectively.

4. Hiatus

Through the detailed observations of coring, thin sections, cathodoluminescence, and the data from scanning electron microscopy and geochemistry, this study found 2 erosion interfaces located at the top of Member Fei 1 and Fei 2, respectively. The characteristics of the lower and upper interfaces are similar, and in the following section, the typical characteristics are described.

4.1. Characteristics of cores

4.1.1. Dissolved fractures, caves, and karren

The core observations revealed that a number of karst identification marks developed in the carbonate layers at the top of Member Fei 1 and Fei 2 respectively in the Puguang Gas Field, such as dissolution fractures, karst caves, and karrens (Figures 2a–2c). Longitudinal dissolution fractures, expanded dissolution fractures, grooves, and small caves were found perpendicular to the karst layers. These caves range from 1 to 2 cm in width and 5 to 30 cm in length. The fillings found in those karst spaces are dominated by carbonaceous mud, along with other mixed seepage materials, such as carbonate sand and calcite. The morphology of the filling substances is commonly irregular, generally observed as vesicles or veins that are perpendicular or nearly perpendicular to the surrounding rocks. The erosional contact with the surrounding rocks is clear and appears to be the product of karst zones with vertical seepage (Figures 2d and 2e). The small- and medium-sized caves are mostly horizontal (Figure 2f), with heights of 2–30 cm, and are filled with coarse-grained calcite or megacrysts (Figures 2c, 2f, and 2g), cave colluvium, and a small amount of sand and mud. The material is semifilling or filling and appears to be the product of horizontal undercurrent karst zones (Luo et al., 2010). Because the caves are dominated by semifilling or filling material, and the scale is relatively small, there was no venting or dropout phenomena during drilling.

The distribution characteristics of the dissolution fractures, karren, and karst caves and the relationship between fracture-cave fillings and surrounding rocks are clear in the Feixianguan Formation. In the vertical direction, dissolution fractures, karren, and karst caves are distributed such that dissolution fractures and grooves are located in the upper part and dissolution pores and

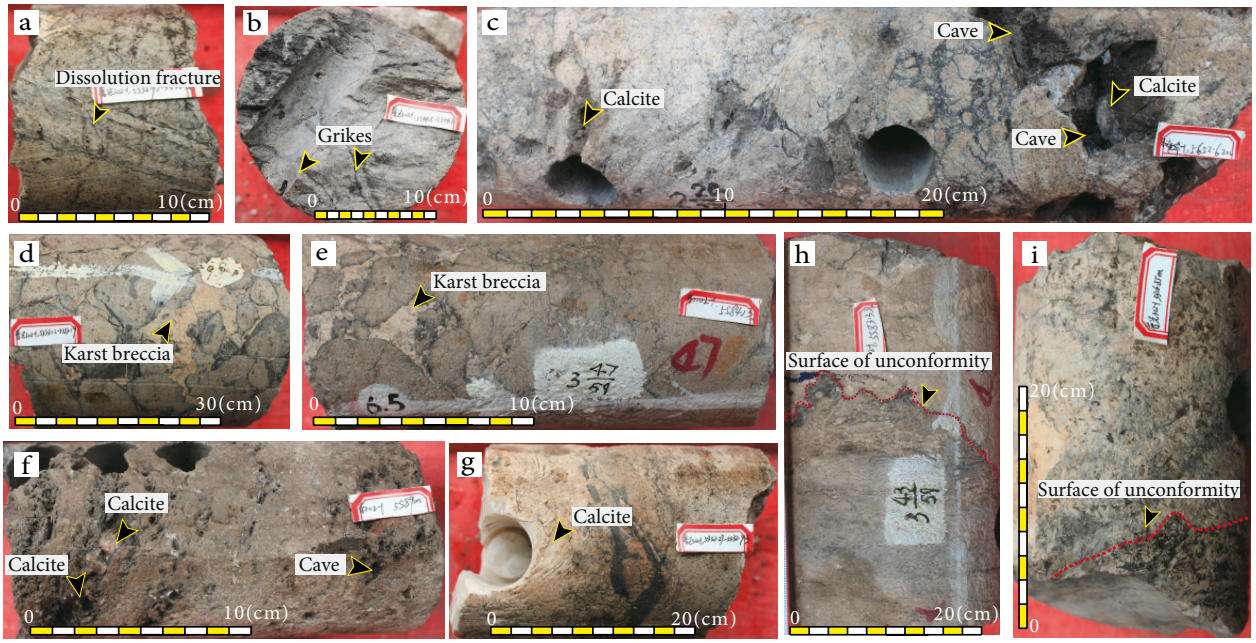

Figure 2. The core-based identification of unconformity interfaces in Puguang Gas Field, northeastern Sichuan: **a)** PG 302-1 well at 5332.97 m (Member Fei 1), exhibiting oolitic dolomite and nearly vertical development of dissolution fractures; **b)** PG 302-1 well at 5344.8 m (Member Fei 1), exhibiting oolitic dolomite and karren filled with oolites; **c)** PG 104-1 well at 5652.62 m (Member Fei 2), exhibiting oolitic dolomite and the development of karst breccia and caves, which are filled with calcite and bitumen; **d)** PG 302-1 well at 5333.12 m (Member Fei 1), exhibiting oolitic dolomite and the development of karst breccia, with gravels that are subangular to angular; **e)** PG 102-1 well at 5584.13 m (Member Fei 2), exhibiting oolitic dolomite and the development of karst breccia, with gravels that are subangular to angular; **f)** PG 102-1 well at 5589 m (Member Fei 1), exhibiting oolitic dolomite and the development of mostly horizontal caves that are not filled to semifilled with calcite; **g)** PG 302-1 well at 5332.27 m (Member Fei 1), exhibiting oolitic dolomite and large caves that are fully filled with calcite; **h)** PG 102-1 well at 5583.33 m (Member Fei 2), where the lower part of the unconformity interface is oolitic breccia with the development of karst breccia, the upper part is micritic dolomite (a dense rock without pore development), and there is interlocking contact between the strata on both sides; **i)** PG 302-1 well at 5316.85 m (Member Fei 1), where the lower part of the unconformity interface is oolitic breccia with pore development, and the upper part is micritic dolomite, a dense rock without pore development. There is interlocking contact between the strata on both sides.

cavities in the lower part. This pattern is the consequence of vertical zonation of karsts. The material that fills the dissolution fractures and karren has a different lithology from the wall rock. The dissolved fractures and karren are produced vertically or near vertically, exhibiting an oblique crossing relationship with the stratification and bedding of the surrounding rocks.

4.1.2. Karst breccia

Karst breccia is one of the important indicators that identify the presence of paleokarst (Gale and Gomez, 2007; Flügel, 2010). The 4 cored wells in the study area revealed the development of massive breccias in the Feixianguan Formation. Examples include the interval at a depth of 5583–5592 m in well PG 102-1 and 5305–5363 m in well PG 302-1 (Figures 2d and 2e). The gravel content in the breccias is 30%–55%, and the gravel diameter is 1.5–13 cm. The gravels, dominated by micritic dolomite and angular to subangular in shape, may result from the endogenous breccias in the Feixianguan Formation. The gravels were cut and surrounded by a network of dissolution fractures that are filled with dark seepage substances, and the dissolution made it difficult for the borders of adjacent breccias to come together. The degree of brecciation gradually decreases downward until it disappears completely.

4.1.3. Karst unconformity

The karst unconformity was formed by the exposure of a large area of early strata due to either a major drop in sea level or tectonic movement (Chen et al., 2007). Based on the core observations from the 4 cored wells and the regional distribution of the well locations, the surface of the unconformity is uneven. The unconformity is typically relatively developed and on the platform margins, whereas the upper and lower strata of the platform interior appear to mostly be in conformable contact. The lithology changes considerably above and below the unconformity surfaces. In general, the strata underlying the unconformity surface are oolitic dolomite with well-developed pores, whereas

the overlying strata are micritic dolomite, a dense rock that generally cannot form effective reservoirs. The strata on both sides of the interface exhibit an interlocking contact that is a clear characteristic of karst unconformity (Figures 2h and 2i).

4.2. Microscopic features

The observation of cast thin sections indicates that there is a powder-fine crystalline dolomite with residual oolitic structure, including faintly visible oolite ghosts (Figures 3a and 3b) beneath the unconformity. Additionally, a geopetal microstructure has developed inside some moldic pores (Figure 3c). This evidence established the presence of karst unconformities (Qiang, 2007). In addition, microscopic observation reveals the development of massive moldic pores and intragranular dissolution pores near the unconformity interfaces (Figures 3c and 3d). These observations reflected the fact that, in the past, the strata had been exposed to a meteoric water environment, where they experienced leaching by meteoric water or dissolution by mixed meteoric water and seawater, causing the selective formation of intragranular dissolution pores (including moldic pores). Cathodoluminescence analyses indicated that the powder-fine crystalline dolomite in the oolitic dolomite near the unconformity interface glows dark red, brown, and purple (Figures 3e and 3f), which are distinct characteristics of meteoric water impact (Huang, 1990). All of these observations, in conjunction with the aforementioned core observations, indicate the presence of karst unconformity.

4.3. Geochemical characteristics

4.3.1. C and O isotopes

C and O isotope analyses were performed for well PG 302-1 at 5100–5400 m. As shown in Figure 4, $\delta^{13}C$ in oolitic dolomite is generally distributed in the range of 1.8‰–3.5‰, and the average is 2.4‰. $\delta^{18}O$ is generally between –1.9‰ and –5.4‰, and the average is –3.8‰.

The correlation analysis of C and O isotopes indicates that, as shown in Figure 4, there is a relatively good correlation between the 2 isotopes, which reflects the impact of diagenesis (Glumac and Spivak-Birndorf, 2002). As discussed above, both C and O isotope data are generally in the range of normal seawater, and none of the O isotope values were lower than –10‰, which indicates that the diagenetic process was essentially not affected by deep-source hydrothermal processes (Kaufman and Knoll, 1995). Therefore, based on the combination of the negative drift of C and O isotopes near the 2 interfaces of Fei 1 and Fei 2 and the aforementioned features of the core and microscopic observations, we conclude that the covariation of C and O isotopes reflects dissolution by meteoric water.

The $\delta^{13}C$ value of Triassic seawater is generally 0‰–1.5‰ (Veizer and Hoefs, 1976). Comparison with the $\delta^{13}C$ values of 1.8‰–3.5‰ measured in this experiment, which are larger than the C isotope value in seawater, indicates that the overall fluids in the study area were more salty than seawater at the time of diagenesis (dolomitization) (Veizer and Hoefs, 1976). Detailed analysis, as shown in Figure 4, reveals that the C isotope values of well PG 302-1 between 5148 m and 5160 m (the top of Fei 2) and 5305 m and 5364 m (the top of Fei 1) are significantly smaller than the C isotope value in the upper and lower segments, which indicates that the aforementioned 2 segments very likely received an input of meteoric water in the generally salty environment of diagenetic fluids (Meyers et al., 1997), reflecting the characteristics of hiatuses.

As for the O isotope, the $\delta^{18}O$ of carbonate is affected by several factors, such as seawater temperature and salinity, and it experienced strong transformation by the subsequent diagenesis. Therefore, the magnitude of $\delta^{18}O$ reflects the relative strength of transformation by late diagenesis (Anderson and Arthur, 1983). As shown in Figure 4, the $\delta^{18}O$ value is reduced in the section between 5305 m and 5364 m, which can be interpreted as the result of the gradually decreasing salinity or increasing temperature of diagenetic fluids (Machel and Lonnee, 2002), or the input of freshwater (Hardie, 1987). When combined with the trend of variation of the C isotopes, our analysis indicated that this effect was primarily caused by a gradual decrease in the salinity of diagenetic fluids due to freshwater input.

4.3.2. Sr isotopes

The $^{87}Sr/^{86}Sr$ values for the oolitic dolomite of the Feixianguan Formation examined in this study are indicated in the Table and in Figure 5. Its value is generally distributed from 0.707536 to 0.707934 (average: 0.707797).

As shown in Figure 5, the $^{87}Sr/^{86}Sr$ value does not vary significantly in well PG 302-1; the data are relatively concentrated between 5305 m and 5364 m with all values greater than 0.7076. Huang (1997) determined the variation range for seawater during the Feixianguan Period of the Early Triassic to be 0.707330–0.707507 in northeastern Sichuan, with an average of 0.707399, which indicates that in this section of depth, the Sr isotope value is significantly higher than that of the seawater in the Feixianguan Period of the Early Triassic.

Meredith and Egan (2002) proposed that the $^{87}Sr/^{86}Sr$ value does not undergo fractionation when the minerals are deposited from fluids, and the $^{87}Sr/^{86}Sr$ value thus remains unchanged throughout the geological history (without experiencing subsequent fluid transformation, such as by hydrothermal fluid and meteoric water) after carbonate minerals are deposited from fluids, which then reflect the $^{87}Sr/^{86}Sr$ value of the fluids upon deposition. Sr isotopes are sensitive indicators of changes in sea level (Huang, 1997), which negatively correlated with variation in the $^{87}Sr/^{86}Sr$

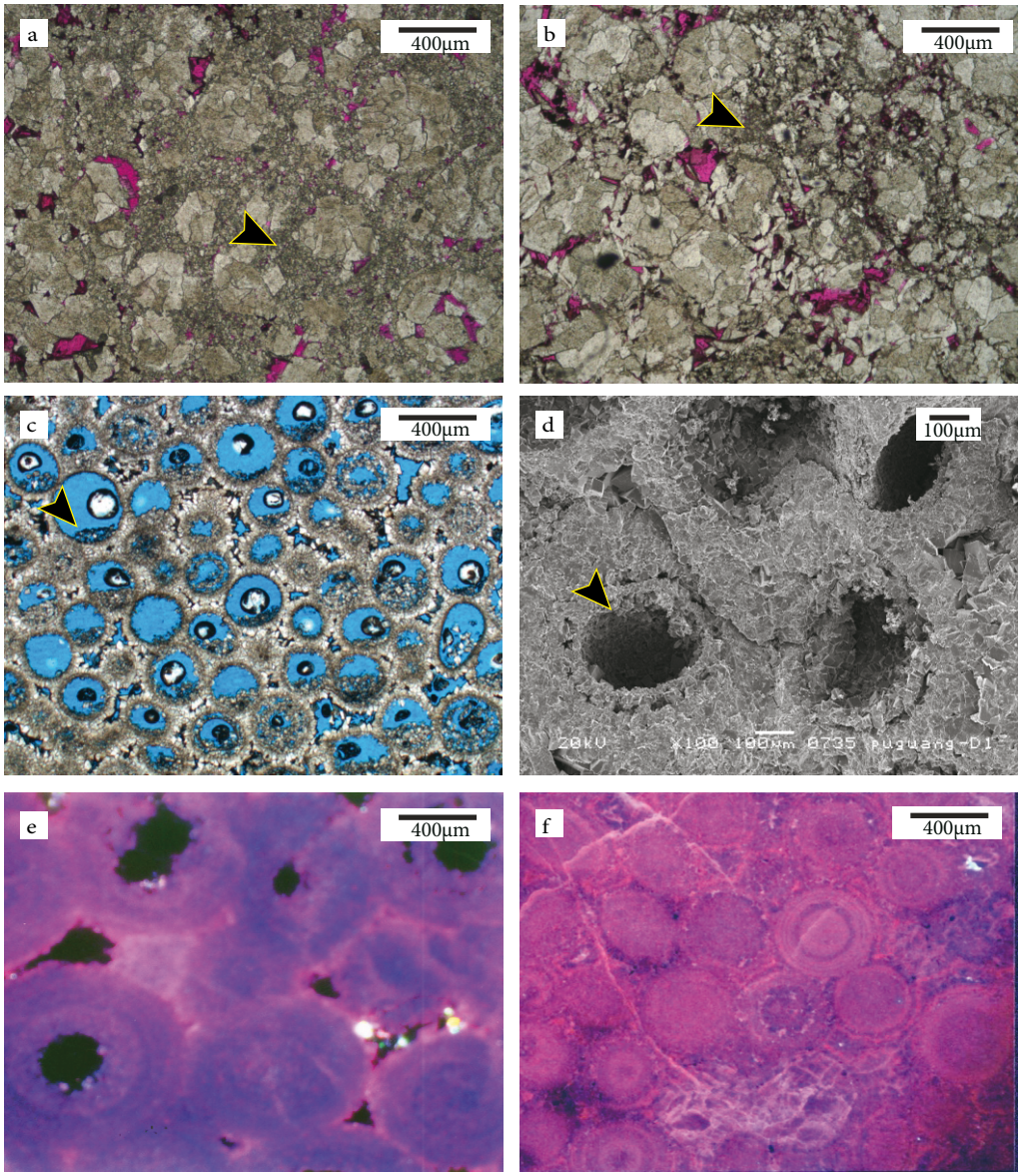

Figure 3. Microscopic pictures of Feixianguan Formation in Puguang Gas Field in northeast Sichuan: **a)** PG 104-1 well (5726.16 m, Member Fei 1), exhibiting residual oolitic fine-grained dolomite, the development of intragranular pores and intergranular dissolution pores, and intergranular (dissolution) pores filled with vadose silt, cast of a filling of vadose silt; **b)** PG 302-1 well (5325.24 m, Member Fei 1), exhibiting residual oolitic fine-grained dolomite and intergranular dissolution pores filled with vadose silt, where the intergranular dissolution pores are divided into a network, cast of a filling of vadose silt from PG 302-1 well; **c)** PG 102-1 well (5586.72 m, Member Fei 2), exhibiting sparry oolitic dolomite with the development of oolitic moldic pores and then intergranular pores, cast of a moldic pore from PG 102-1 well (5586.72 m, Member Fei 2); **d)** PG 102-1 well (5584.64 m, Member Fei 2), exhibiting sparry oolitic dolomite with the development of oolitic moldic pores and then intergranular pores, electron microscopy of a moldic pore from PG 201-1 well; **e)** PG 104-1 well (5720.36 m, Member Fei 1), exhibiting residual oolitic dolomite with pore development mainly involving the formation of intergranular dissolution pores, where the dolomite glows purple in cathodoluminescence (40×, CL); **f)** PG 102-1 well (5587.5 m, Member Fei 2), exhibiting sparry oolitic dolomite with the development of intragranular pores, where the dolomite glows purple in cathodoluminescence (40×, CL).

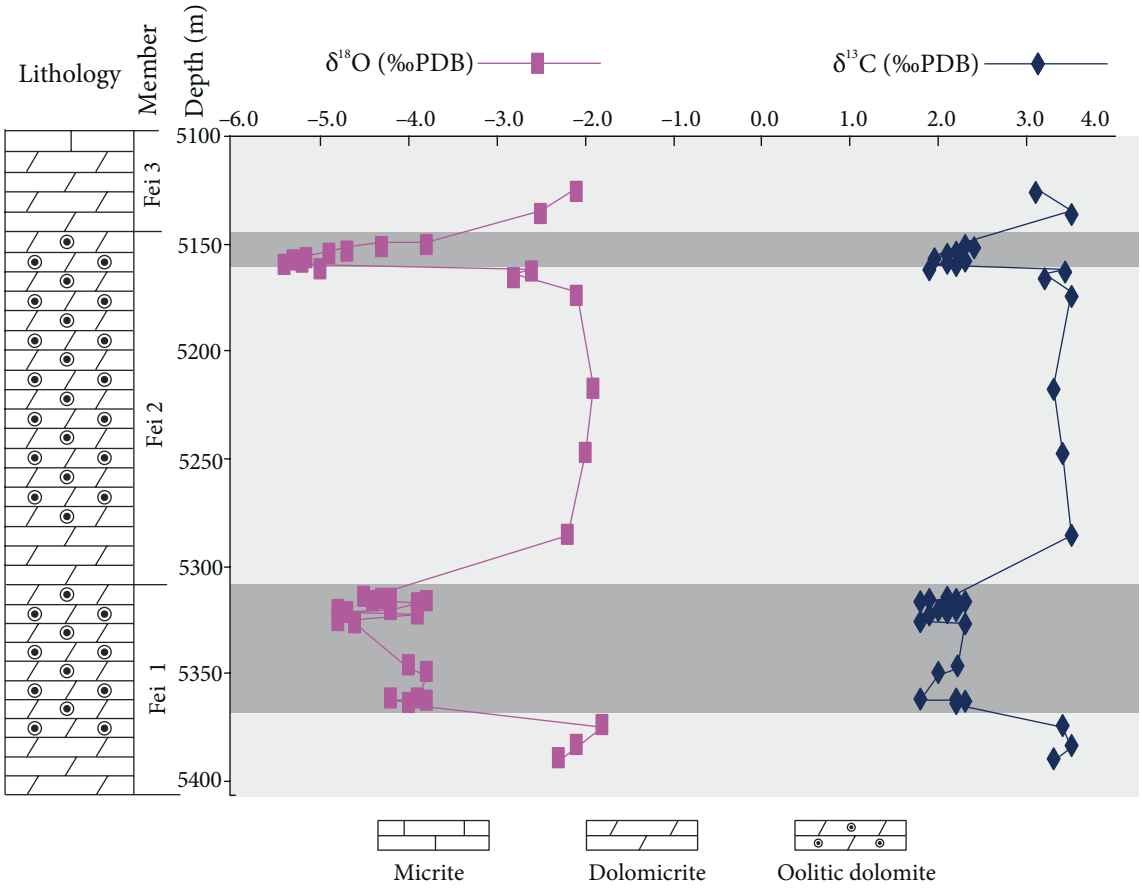

Figure 4. The C and O isotope analysis for the Feixianguan Formation based on well PG 302-1 and a diagram of the relationship between $\delta^{18}O$ and $\delta^{13}C$.

ratio (Li et al., 2000). The addition of terrigenous Sr can cause relative increases in the $^{87}Sr/^{86}Sr$ ratio in seawater. Moreover, Azmy et al. (2001) suggested that fluids in the silicate stratum that participate in dolomitization can also result in higher $^{87}Sr/^{86}Sr$ ratios than seawater in the same period.

As shown in Figure 5, the $^{87}Sr/^{86}Sr$ ratio in the depth section of 5305 m to 5364 m in well PG 302-1 is greater than the $^{87}Sr/^{86}Sr$ ratio in the seawater of the same period, and the samples measured were all dolomite. This discrepancy can be attributed to the impact of the addition of terrigenous Sr or the fluids from silicate formation participation in dolomitization. Huang et al. (2011) proposed that the participation of fluids related to aluminum silicate in dolomitization must be supported by the characteristics of "high Mn and low Sr", but the average Mn content in dolomite in the interval at depths of 5305–5364 m in the study area is only 48.11×10^{-6}, and the average Sr content is only 73.11×10^{-6} (Table). Thus, both characteristics are low. Therefore, the higher $^{87}Sr/^{86}Sr$ value for dolomite at this depth interval compared with the seawater in the same period was mainly caused by the addition of terrigenous Sr. Usually, tectonic uplift can cause a relative decrease in sea level, which causes an increase in the terrigenous Sr carried by continental weathering into the ocean, resulting in a relative increase of the $^{87}Sr/^{86}Sr$ value in seawater (Yan et al., 2005). Consequently, the Sr isotopic characteristics also indicate the occurrence of a hiatus interface near the top of Fei 1.

The aforementioned geochemical characteristics indicate that the strata on the tops of Fei 1 and Fei 2 were briefly exposed to the atmosphere, where they experienced meteoric transformation and dissolution. Typically, exposed strata will be dissolved and transformed by meteoric water for 1 of 2 reasons. The first reason for exposition would be an absolute decrease in sea level, and the second is a relative decrease in sea level caused by tectonic uplift. At the plateau margin of the Changxing Formation-Feixianguan Formation in the Puguang area, the magnitude of sea level variation is not large; thus, absolute decreases in sea level are unlikely to play a role. In addition, the study of Guo et al. (2012) on well PG 2 also found the development of meteoric dissolution on the tops of Fei 1 and Fei 2. Although the PG 302-1 and PG 2 wells

Table. Analysis of Sr isotopes and major and trace elements in carbonates of the Feixianguan Formation of the Lower Triassic in well PG 302-1.

Depth (m)	$^{87}Sr/^{86}Sr$	2σ (± ×10^{-5})	MgO%	CaO%	Sr (×10^{-6})	Mn (×10^{-6})	Fe (×10^{-6})
5283.63	0.70753555	0.000013	17.82	35.21	279.00	36.38	3277.83
5297.68	0.70754761	0.000010	18.37	34.27	563.45	35.49	2999.36
5314.55	0.70778946	0.000011	20.93	33.51	81.20	41.53	1785.29
5315.25	0.70775181	0.000015	20.76	31.91	49.70	42.29	1728.55
5315.95	0.70775098	0.000013	21.61	32.26	58.10	46.91	1738.14
5316.32	0.70777539	0.000010	21.47	31.12	63.10	57.39	3888.22
5316.90	0.70776342	0.000012	21.38	31.94	91.80	66.91	2391.91
5317.02	0.70776919	0.000009	21.25	33.78	80.70	48.12	1833.41
5317.32	0.70779570	0.000010	21.10	32.45	71.30	41.53	1981.76
5317.92	0.70769070	0.000011	20.69	33.49	93.40	50.56	1779.16
5320.60	0.70784031	0.000012	20.83	32.17	90.70	44.80	1904.34
5321.83	0.70788332	0.000010	21.86	32.42	56.80	44.76	1947.45
5322.83	0.70781931	0.000011	21.13	32.88	61.50	42.97	1850.84
5325.97	0.70793417	0.000009	20.70	33.21	72.80	45.24	2144.85
5326.95	0.70789137	0.000011	20.90	32.93	59.90	54.85	1837.87
5362.01	0.70784734	0.000012	20.62	32.16	73.50	58.94	1895.92
5362.65	0.70781614	0.000010	20.76	33.93	71.70	46.02	2005.33
5363.40	0.70781425	0.000012	20.40	33.12	75.80	52.87	3420.29
5364.45	0.70752041	0.000008	20.56	32.39	81.80	37.33	1779.38
5364.85	0.70744924	0.000021	21.66	32.12	78.30	34.67	1622.74

are both located on the platform margin, the elevations of these 2 wells differ by 234.41 m (585.43 m above sea level for PG 302-1 and 351.04 m above sea level for PG 2), and an absolute decrease in sea level on a scale of this magnitude is highly unlikely. Therefore, it is preliminarily concluded that dissolution and transformation of exposed strata in the study area by meteoric water were primarily caused by relative declines in sea level due to tectonic uplift, resulting in the creation of a hiatus.

5. Geological significance

5.1. Phases of Indosinian tectonic cycles

The tectonic period between the Late Permian and Triassic (257–205 Ma) was an important Indosinian tectonic period. During this period, Indosinian movement occurred in China and the surrounding regions. A great deal of research has examined the tectonic episode divisions of Indosinian movement. Zhang (1958) examined Indosinian movement in southern China and suggested that 3 crustal movements occurred during the Triassic (at the end of the Early Triassic, after the Carnian and before the Norian, and from the end of the Triassic to the early Jurassic). Based on these crustal movements, the Indosinian movement may be divided into the 3 corresponding episodes of the Lower Yangtze movement, the Huaiyang movement, and the Nanxiang movement (Figure 6). Ren (1984) proposed that the Indosinian orogenic cycle may be divided into the following 3 episodes of important tectonic movements in the Indosinian geosynclinal area of southwestern China: the first episode occurred from the late Ladinian to the early Carnian, the second episode occurred between the early and middle Norian, and the third episode occurred from the late Rhaetian to the beginning of the Hettangian. In combination, these episodes represent a complete orogenic process from the late Middle Triassic to the early Jurassic (Figure 6). Deng et al. (1980) conducted a detailed examination of deposition and tectonic deformation during the Indosinian movement in the Lower Yangtze region and proposed that the Jinzi movement and the Nanxiang movement (Figure 6) may have occurred in the study area. The aforementioned investigations demonstrated the division of the Indosinian movement into 3 episodes with good agreement on the eras assigned to each episode.

However, certain scholars have proposed dividing the Indosinian movement into 4 episodes. For example,

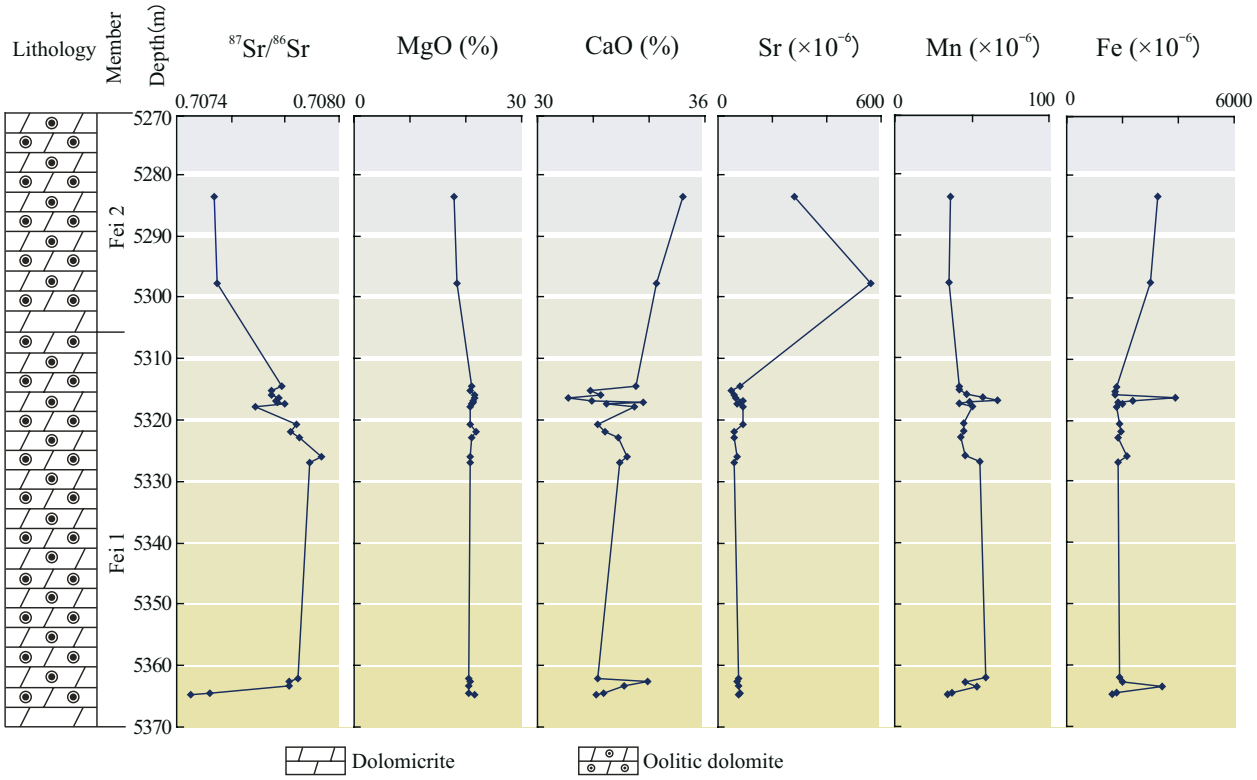

Figure 5. Distribution of $^{87}Sr/^{86}Sr$ values with depth in well PG 302-1.

Mei (2010) divided the upper Yangtze movement into 4 episodes, with the first episode occurring in the late Early Triassic, the second during the Late Middle Triassic, the third before the Rhaetian, and the fourth at the end of the Triassic (Figure 6).

In accordance with the findings of previous studies, this study found 2 distinct unconformable interfaces in the Lower Triassic Feixianguan Formation; these interfaces represent 2 separate tectonic events. Based on these findings, references to previous division schemes, and the premise of maintaining the existing scheme of dividing the Indosinian movement into 4 episodes, the first episode of the Indosinian movement is divided into the following three subepisodes: the first subepisode, the second subepisode, and the third subepisode (Figure 6). The first 2 subepisodes of the first episode of the Indosinian movement play a particularly significant role in the study area.

Regional tectonics indicate that the first 2 subepisodes of the first episode of Indosinian movement in the study area were closely related to a collision between the South Qinling orogenic belt and the Yangtze plate (Xu et al., 2012). The study area is located on the northern margins of the upper Yangtze plate, south of the Micang Mountains and north of the Qinling orogenic belt (Figure 1b). The deposition and tectonics of this area are affected by Qinling orogenic processes; conversely, the deposition and tectonic evolution of the study area may also reflect Qinling orogenic processes. Research addressing sedimentary tectonics in the study area prior to the initial collision between the South Qinling orogenic belt and the Upper Yangtze block has mainly focused on 2 periods, the Ladinian of the Middle Triassic (approximately 237–228 Ma, after the deposition of the Leikoupo Formation) (Meng et al., 2005) and the Norian of the Late Triassic (approximately 216.5–203.6 Ma, during the deposition of the Xujiahe Formation) (Yin and Nie, 1993). However, Chen et al. (2010) studied an unconformable Lower Triassic internal interface in the Micang Mountains in northern Sichuan and suggested that the South Qinling orogenic belt and the Upper Yangtze block collided during the Olenekian of the Early Triassic (approximately 249.7–245.0 Ma). These researchers also proposed that the Olenekian is simply the earliest time during which a collision between the South Qinling orogenic belt and the Upper Yangtze block was evident in this particular study area; the initial collision may actually have occurred earlier, during the era in which the Kaijiang-Liangping trough developed.

This study indicates that, during the Induan of the Early Triassic (approximately 251–245.0 Ma), 2 tectonic uplifts occurred in the study area, forming 2 unconformable interfaces. These 2 unconformable

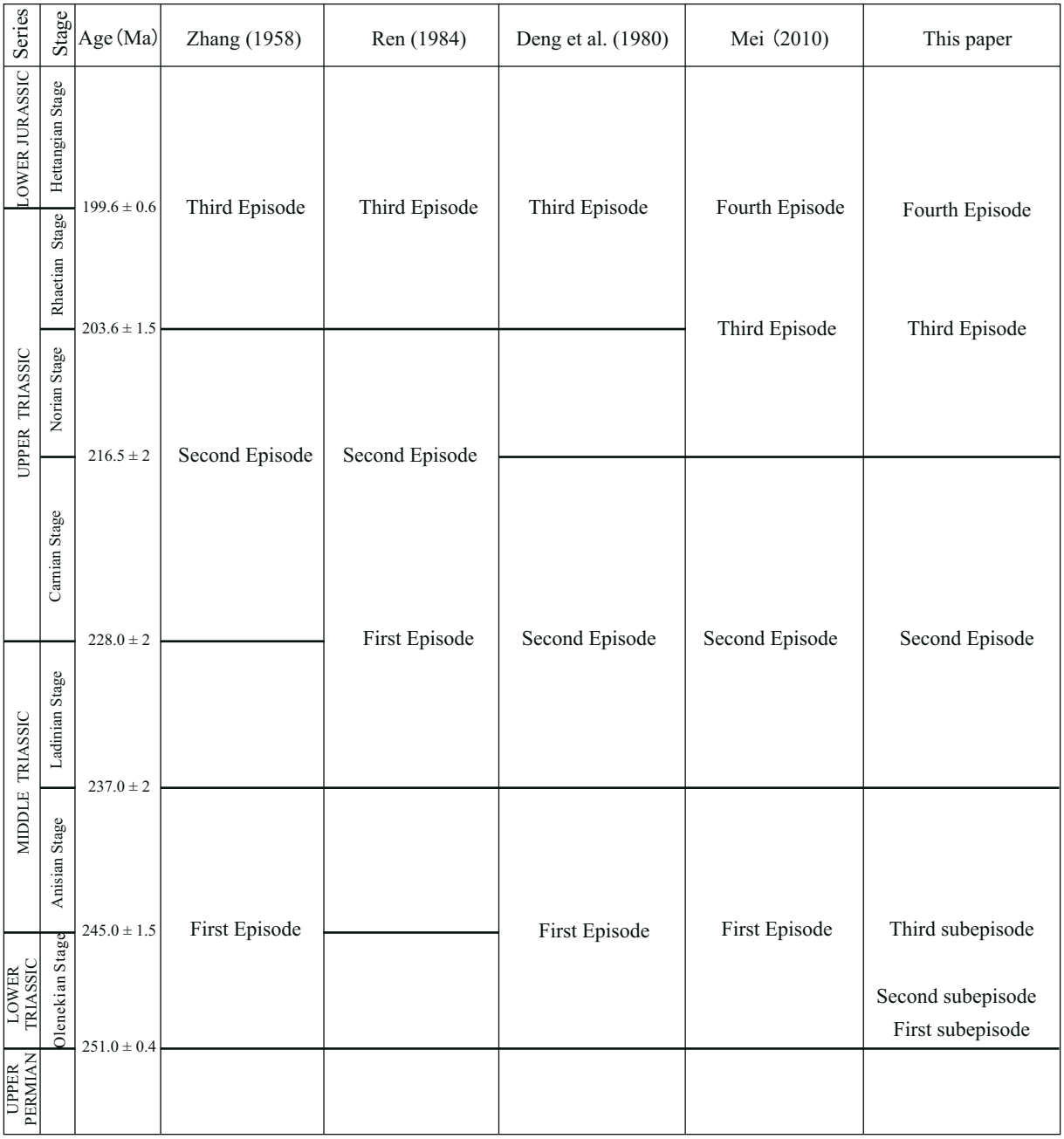

Figure 6. Comparison of different subdivisions of the Indosinian movement into tectonic episodes.

interfaces have both been observed in outcrops of other regions in the northeastern Sichuan Basin (Figure 1a). These observations clearly illustrate that these 2 tectonic uplifts were regional. The combination of these results with the sedimentary tectonic characteristics of the region suggests that these 2 tectonic events were related to the Qinling collisional orogeny. In other words, during the Induan of the Early Triassic, the South Qinling orogenic belt collided with the Yangtze block, and the resulting tectonic deformation affected the northern margin of the Yangtze block. This timing is essentially consistent with the initial collision time suggested by Chen et al. (2010). Notably, the Induan is the main period during which the Kaijiang-Liangping trough developed (Wang YG et al., 2002).

5.2. Sequence interface divisions

Many prior studies have examined the sequence of strata in the Feixianguan Formation of Sichuan Basin. For instance, Chen (1995) divided the Changxing Formation and Feixianguan Formation into the same

third-order sequence; Chen et al. (2009) divided the Changxing Formation-Feixianguan Formation into 4 third-order sequences, with 2 third-order sequences for each formation; and Guo (2011) divided the Feixianguan Formation in northeastern Sichuan into 2 third-order sequences, which correspond to Fei 1–Fei 2 and Fei 3–Fei 4. Thus, it is evident that there are differences between the various division schemes proposed for this region.

In this paper, based on the findings of previous studies, research regarding the sequences of the Feixianguan Formation in northeastern Sichuan was furthered through the identification of the hiatus interface of this formation. The Feixianguan Formation was divided into 2 third-order sequences (Figure 7), which are referred to as the lower sequence, middle sequence, and upper sequence. The bottom interface of the lower sequence is the interface between the Feixianguan Formation and the Changxing Formation, and the top interface of this sequence is the interface between Fei 1 and Fei 2. The top interface of the middle sequence is the interface between Fei 2 and Fei 3, and the top interface of the upper sequence is the interface between the Feixianguan Formation and the Jialingjiang Formation.

It is well known that sequence interfaces include 2 different types of interfaces, namely unconformable and conformable interfaces (Mei, 1995). Consequently, unconformable interfaces can be used as a basis for sequence interface divisions that can guide the division of sequences in a study area, eventually allowing a unified isochronous interface to be identified for the division of internal sequences in the Feixianguan Formation of the study area. In the aforementioned sequence interfaces for the Feixianguan Formation, exposed unconformable interfaces typically occur between Fei 1 and Fei 2 as well as between Fei 2 and Fei 3. Therefore, in the division of the sequence interfaces and the sequence of strata for the Feixianguan Formation, there should be 3 third-order sequences that correspond to Fei 1, Fei 2, and Fei 3–Fei 4.

In the Feixianguan Formation, the typical exposed unconformable interfaces in the study area exhibit evidence of sediments that experienced exposure, causing karstification. Core observations allowed the characterization of the vertical lithologic development of Member Fei 1 and Member Fei 2 in the Feixianguan Formation. The rock types of the middle and lower portions of Member Fei 1 are primarily micritic limestone and marl, whereas the upper portion of Member Fei 1 generally develops oolitic shoals and exhibits signs of karstification. Micritic dolomite developed in the lower portion of Member Fei 2, whereas oolitic shoals developed in the middle and upper portions of this member, with signs of karstification present in the upper portion.

5.3. Reservoir quality

Various types of carbonate pores exist below unconformable interfaces; typically, these regions feature the development of internal moldic pores and cavities, fractures increased by dissolution, and breccia pores among other pore types (Fan, 2005). A large quantity of research data indicates that many domestic and international oil and gas basins are located in unconformity interface-related reservoir rocks, such as the Anadarko Basin (Mazzullo, 1995), Williston Basin (Lucia, 1999), and Permian Basin (Lucia and Kerans, 2003) in the United States; the Ordos Basin in China (Wang ZC et al., 2002); the Natih and Fahud oil fields of Oman (Alsharhan and Scott, 2000); and the Bu Hasa oil field of the United Arab Emirates (Alsharhan, 1987). The above examples indicate that strata below an unconformity interface typically experience weathering erosion and dissolution leaching. These processes can significantly improve the capacity of reservoirs and play an important constructive role in reservoir formation. However, in the study area, microscopic observations and examinations of well log interpretations revealed that the unconformable interfaces (between Fei 1 and Fei 2 and between Fei 2 and Fei 3) in the Feixianguan Formation may play a relatively destructive role with respect to the petrophysics of high-quality reservoirs.

The core and microscopic observations of sequences at the top of the Member Fei 1 and Member Fei 2 respectively reveal typical characteristics of exposed settings. This indicates that the study area experienced 2 brief uplifts and was subjected to leaching and dissolution by meteoric water. The dissolution of unstable minerals at the top of the exposed regions caused the formation of intragranular dissolution pores and moldic pores. During the same period, vadose silt filled the lower portions of the vadose zone. As the silt debris filled in the primary and secondary dolomite pores, the pore network of reservoirs changed. On one hand, vadose silt was distributed throughout pores, occupying the original reservoir space and thereby decreasing reservoir porosity; on the other, this silt redivided the inter- and intragranulate dissolution pores into many small pores to a certain extent, and thereby decreased reservoir permeability (Figures 3a and 3b). As the graph of well log interpretation shows (Figure 8), it is evident that these reservoirs remained effective, though vadose silt strikingly reduced the porosity and permeability of reservoirs in the karstification zone.

In addition, with respect to cementation associated with dissolution, total porosity typically does not increase during periods of surface exposure for carbonate sediments affected by diagenesis in freshwater and mixed zones (Halley and Evans, 1983; Scholle and Halley, 1985). In fact, in many situations, total porosity actually decreases during these times (Harrison, 1975; Walkden and Williams,

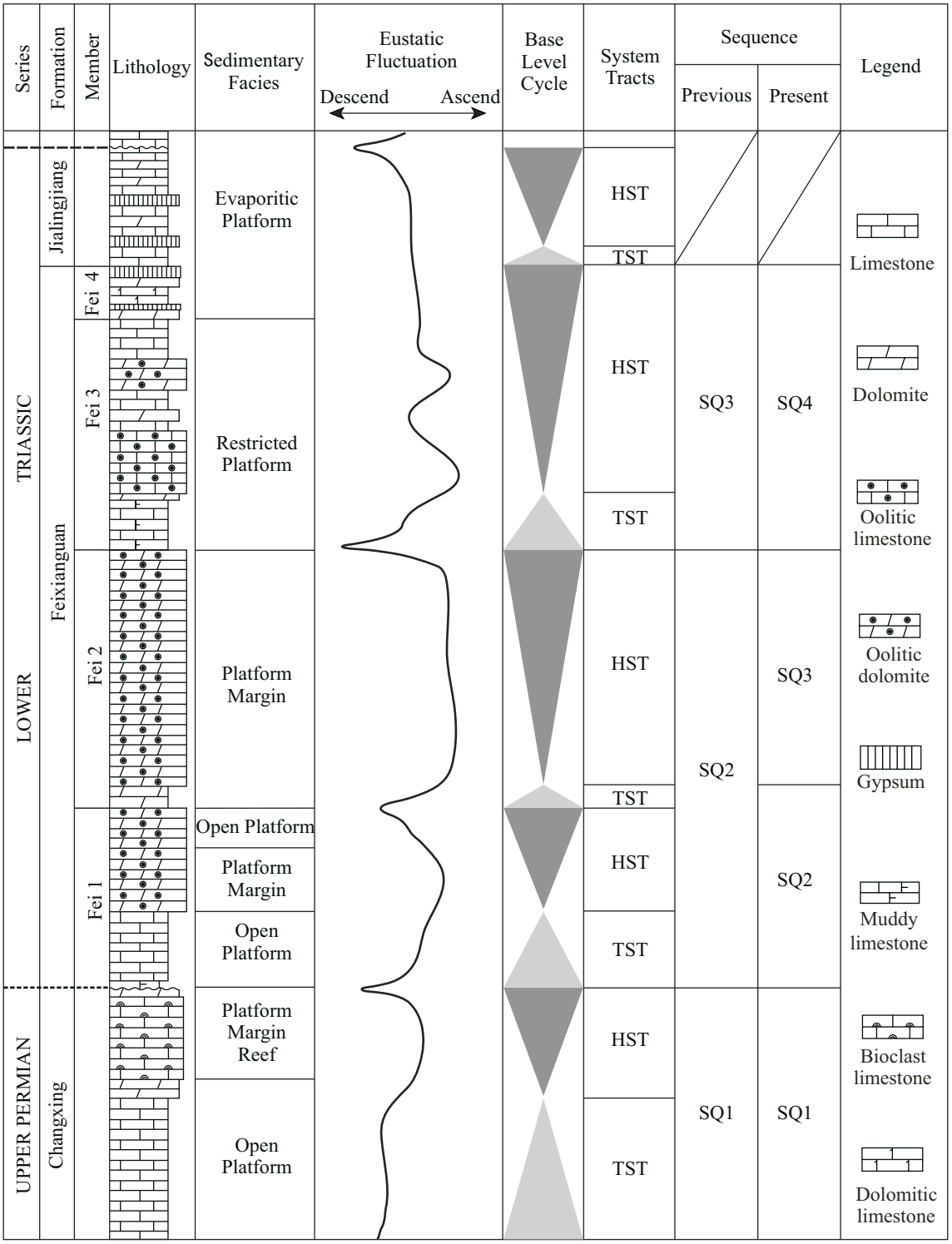

Figure 7. The sequence of the Feixianguan Formation in the Puguang Gas Field.

1991). Although secondary pores form during surface exposure periods, localized to widespread cement plugs often fill the original pores of exposed rock (particularly the primitive pores) (Hird and Tucker, 1988; Walkden and Williams, 1991). The microscopic observations of oolite shoal reservoirs of the Feixianguan Formation in the study area reveal 3 phases of cementation. The first phase occurred in the marine environment, the second phase

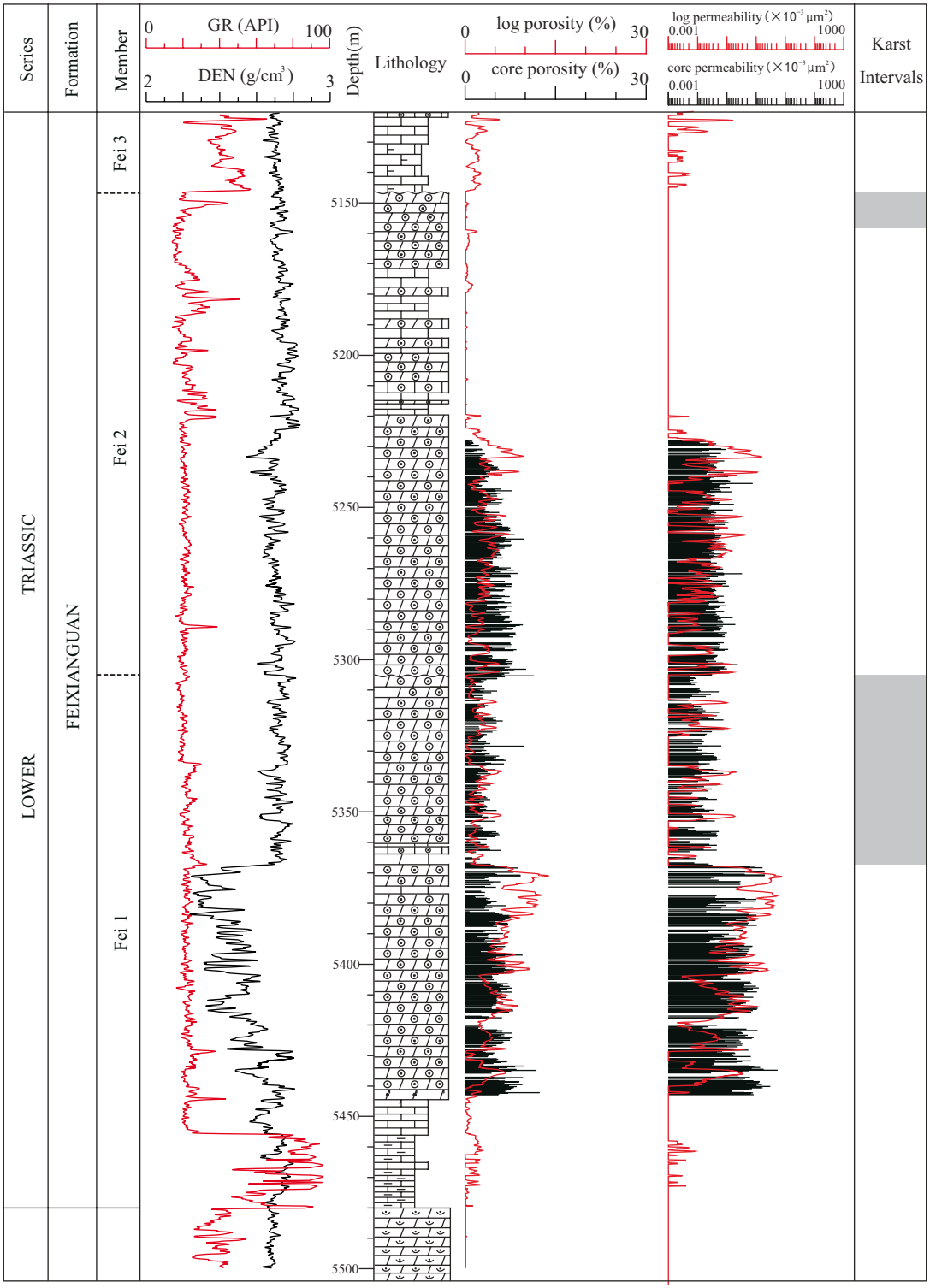

Figure 8. Log interpretation for well PG 302-1.

primarily occurred in the meteoric water environment, and the third phase occurred in the buried diagenetic environment. In particular, due to the impact of the second phase of cementation, primary pores may decrease by 80%–100% (Wang et al., 2010). This phenomenon mainly occurred because, after the deposition of oolitic shoals, tectonic uplift caused the relative decline of sea levels. At this time, oolites were mainly composed of

aragonite and high-magnesium calcite, which are stable minerals in the marine environment but unstable minerals when exposed to meteoric water. The meteoric water easily selectively dissolved these unstable minerals to form oolitic moldic pores and intragranular dissolution pores. Calcium carbonate generated by aragonite dissolution then reprecipitated on particle surfaces to form thick, ring-shaped cement that caused varying degrees of damage to the original intergranular pores. Thus, in the section of the study area featuring the development of oolitic moldic pores and intragranular dissolution pores, there is a clear pattern of cementation between particles, and the original intergranular pores have essentially been completely filled.

5.4. The causes of reservoir formation

Core observations of 4 systematically cored wells in the study area indicated that at the top of Member Fei 1 and Member Fei 2 in the Feixianguan Formation, there existed large dissolution pores with diameters of greater than 2 mm. Previous studies suggested that these dissolution pores were mainly caused by the thermochemical sulfate reduction (TSR) reaction during buried stages of diagenesis (Zhu et al., 2005a, 2005b; Ma et al., 2007a). This speculation was reasonable as the TSR reaction can generate a great deal of H_2S, besides the Puguang Gas Field itself being a dry gas field with high H_2S content. It has been reported that there is approximately 12.7%–17.2% H_2S content of natural gas in this field (Ma et al., 2007b). However, not all gas layers in the Puguang Gas Field belong to high-sulfur gas reservoirs, and a small fraction of them contain gas with no H_2S or only trace quantities of H_2S (Ma, 2008). Based on the results of the present work, we suggest that the large dissolution pores may have arisen primarily through karstification instead of through the TSR reaction.

There are several pieces of sound evidence supporting this suggestion. First, core observations provided vital indicators for the presence of paleokarst, such as karst breccias, unconformable interfaces, karst caves, dissolution fractures, and karrens (Figure 2). In dissolution pores, holes, and fractures, dolomite fillings reflect meteoric effects, whereas the presence of various other fillings, such as terrigenous clasts and vadose silt (Figures 3a and 3b), reflect the occurrence of karstification. Second, core observations of 4 cored wells revealed the distinct zonation of cross-sectional dissolution characteristics, which were mainly distributed across the strata below Fei 1 and Fei 2. These zones developed at a depth of 10–50 m below the top of Fei 1 and Fei 2, respectively, exhibiting characteristics consistent with zonation caused by near-surface water rather than by the TSR reaction. Third, the reservoir spaces between oolitic shoal lithofacies observed in those 4 cored wells of the Puguang Gas Field mainly consist of oomoldic pores, intragranular dissolution pores, and intergranular dissolution pores (Wang et al., 2008). Based on the TSR theory and the evidence of high hydrogen sulfide content in current gas reservoirs of this field, much greater reservoir capacities would be expected to be generated by the occurrence of large-scale TSR reactions in reservoirs during the late stages of buried diagenesis than by the occurrence of dissolution during the early stages of burial. However, according to the observations of more than 4200 thin sections from the Feixianguan Formation and its lower strata, the Changxing Formation in Puguang Gas Field, Xia et al. (2010) found that within these samples, bituminous rims characteristic of H_2S dissolution corrosion were rarely observed inside pores and occurred in only approximately 1%–2% of the total number of pores. This indicates that the reservoir space affected by TSR reaction in this gas field is extremely limited. Guo et al. (2012) conducted simulation experiments to assess the impact of TSR reaction in this reservoir, suggesting that relatively very few pores developed in the late stage of the whole diagenesis process in the study area; besides, fewer pores were produced by the TSR reaction alone.

Based on the analysis above, in combination with core and microscopic observations, preliminary assessments of the current types, morphologies, and filling statuses of reservoir pores in the study area indicate that the TSR reaction was one factor for the formation or transformation of reservoir pores, but not the dominant factor. The large dissolution pores in the oolite shoal reservoirs of the Feixianguan Formation in this area were likely primarily formed by karstification.

6. Conclusions

1) Based on the samples and data from the 4 cored wells in the Puguang Gas Field, northeastern Sichuan Basin, 2 surfaces indicating discontinuous deposition were observed in the internal sequence of the Lower Triassic Feixianguan Formation. Notably, penecontemporaneous weathering crust karstification is the main factor resulting in karst unconformities between weathering surfaces at the top of Member Fei 1 and Member Fei 2, respectively.

2) Core observations indicate the presence of homogeneous oolitic dolomite or limestone above the unconformity interfaces. Under these interfaces, large numbers of dissolution fractures, caves, karrens, and karst breccia developed. The dissolution fractures and karrens were mostly filled by seepage containing a mixture of carbonaceous mud, sand, calcite, and other source material. The caves were generally partially or completely filled with coarse-grained or giant crystalline calcites. The karst breccia contained angular/subangular gravel that was mainly composed of micritic dolomite, which is the endogenous breccia within the Feixianguan Formation.

3) Analyses of cast thin sections demonstrated that

in the underlying strata of the unconformity interface in the study area, residual oolitic structures of powder-fine crystalline dolomite developed with faintly visible oolite ghosts. Inside intergranular pores and dissolution intergranular pores, vadose silt was produced by the vadose zone in the exposed environment during early continental diagenesis, and the degree of vadose silt development gradually decreases with increasing depth from the interface. In addition, cathodoluminescence analyses indicate that the powder-fine oolitic dolomite near the unconformity interfaces glows dark red, brown, and light purple, exhibiting distinct characteristics of meteoric water effects.

4) The assessment of C, O, and Sr isotopes and trace elements indicated that, in the study area, the top layers of both Fei 1 and Fei 2 of the Feixianguan Formation experienced the effects of meteoric water diagenesis. In particular, these effects caused significant decreases in the C and O isotope ratios and significant increases in the Sr isotope ratios in the karst zone. The trace elements Mn and Fe provided suitable conditions for cathodoluminescence assays.

5) The discovery of paleokarst unconformities in the Feixianguan Formation in the study area provided direct evidence clarifying the internal stratigraphic divisions of this formation in the Lower Triassic. First, in the tectonic episode division of the Indosinian movement, the first episode was subdivided into 3 subepisodes. This subdivision reflected the effects of 2 uplifts early in the Indosinian that caused the outcropping of large areas of the platform, resulting in the 2 karst unconformities. Second, the Feixianguan Formation is divided into 3 third-order sequences that correspond to Fei 1, Fei 2, and Fei 3–Fei 4.

6) The development of 2 penecontemporaneous karsts in the Feixianguan Formation in the study area played a dual role in the development of the quality of the reservoirs. Notably, although massive dissolution pores were formed, seepage materials filled existing pores. Nonetheless, on the whole, reservoirs in karstification zones of the study area could generally be classified as effective reservoirs. In addition, based on current theories regarding karsts, it appears that the TSR reaction was not a dominant factor in the formation or transformation of reservoir pores. Instead, large dissolution pores in the region were mainly formed by karstification.

Acknowledgments

We thank the Zhongyuan Oilfield Company for providing data and permission to publish this work. This work was supported by the Major State Basic Research Development Program (973 Project, Grant No. 2012CB214803), a China's National Science & Technology Special Project (Grant No. 2011ZX05017 and No. 2011ZX05049), the PetroChina Research Fund (Grant No. 2011D-5006-0105), and a Key Subject Construction Project of Sichuan Province, China (Grant No. SZD 0414).

References

Alsharhan AS (1987). Geology and reservoir characteristics of carbonate buildup in Giant Bu Hasa oil field, Abu Dhabi, United Arab Emirates. AAPG Bull 71: 1304–1318.

Alsharhan AS, Scott RW (2000). Hydrocarbon potential of Mesozoic carbonate platform–Basin systems, U.A.E. SEPM Spec Publ 69: 335–358.

Anderson TF, Arthur MA (1983). Stable isotopes of oxygen and carbon and their application to sedimentologic and paleoenvironmental problems. In: Arthur MA, editor. Stable Isotopes in Sedimentary Geology. Tulsa, OK, USA: SEPM Short Course Notes, pp. 1–151.

Azmy K, Veizer J, Misi A, de Oliveira TF, Sanches AL, Dardenne MA (2001). Dolomitization and isotope stratigraphy of the Vazante Formation, São Francisco Basin, Brazil. Precambrian Res 112: 303–329.

Chen HD, Zhong YJ, Hou MC, Lin LB, Dong GY, Liu JH (2009). Sequence styles and hydrocarbon accumulation effects of carbonate rock platform in the Changxing-Feixianguan Formations in the Northeastern Sichuan Basin. Oil Gas Geol 30: 539–547 (in Chinese with an abstract in English).

Chen JS, Li Z, Wang ZY, Li L, Ma Q (2007). Paleokarstification and reservoir distribution of Ordovician carbonates in Tarim Basin. Acta Sediment Sin 25: 858–868 (in Chinese with an abstract in English).

Chen ZQ (1995). The late Permian global flooding events. Sediment Facies Palaeogeogr 15: 34–39 (in Chinese with an abstract in English).

Deng YG, Wu RT, Xin JR (1980). The Indosinian movement in lower Yangtze region. Geol Rev 26: 430–435 (in Chinese with an abstract in English).

Fan JS (2005). Characteristics of carbonate reservoirs for oil and gas fields in the world and essential controlling factors for their formation. Earth Sci Front 12: 23–30 (in Chinese with an abstract in English).

Flügel E (2010). Microfacies of Carbonate Rocks: Analysis, Interpretation and Application. 2nd ed. Berlin, Germany: Springer-Verlag.

Gale JFW, Gomez LA (2007). Late opening-mode fractures in karst-brecciated dolostones of the lower Ordovician Ellenburger Group, West Texas: recognition, characterization, and implications for fluid flow. AAPG Bull 91: 1005–1023.

Glumac B, Spivak-Birndorf ML (2002). Stable isotopes of carbon as an invaluable stratigraphic tool: an example from the Cambrian of the Northern Appalachians, USA. Geology 30: 563–566.

Guo CG, Li R, Yang YY, Xie FC, Dong WY (2011). Sequence stratigraphy and evolutionary models for the Changxing Formation in the Tongjiang-Nanjiang-Bazhong zone, Sichuan. Sediment Geol Tethyan Geol 31: 28–32 (in Chinese with an abstract in English).

Guo TL (2011). Sequence strata of the platform edge in the Changxing and Feixianguan formations in the Yuanba area, Northeastern Sichuan Basin and their control on reservoirs. Acta Petrol Sin 32: 387–394 (in Chinese with an abstract in English).

Guo XS, Guo TL, editors (2012). The Exploration Theory and Practice of Carbonate Platform Margin, Puguang and Yuanba Gas Field. Beijing, China: Science Press (in Chinese).

Halley RB, Evans CC (1983). The Miami Limestone: A Guide to Selected Outcrops and Their Interpretation. Miami, FL, USA: Miami Geological Society.

Hardie LA (1987). Dolomitization: a critical view of some current views. J Sediment Res 57: 166–183.

Harrison RS (1975). Porosity in Pleistocene grainstones from Barbados: some preliminary observations. Bull Can Petrol Geol 23: 383–392.

Hird K, Tucker M E (1988). Contrasting diagenesis of two carboniferous oolites from South Wales: a tale of climatic influence. Sediment 35: 587–602.

Huang SJ (1990). Cathodoluminescence and diagenetic alteration of marine carbonate minerals. Sediment Facies Palaeogeogr 4: 9–15 (in Chinese with an abstract in English).

Huang SJ (1997). A study on carbon and strontium isotopes of late Paleozoic carbonate rocks in the Upper Yangtze platform. Acta Geol Sin 71: 45–53 (in Chinese with an abstract in English).

Huang SJ, Huang Y, Lan YF, Huang KK (2011). A comparative study on strontium isotope composition of dolomites and their coeval seawater in the late Permian-early Triassic, NE Sichuan Basin. Acta Petrol Sin 27: 3831–3842 (in Chinese with an abstract in English).

Kaufman AJ, Knoll AH (1995). Neoproterozoic variations in the C-isotopic composition of seawater: stratigraphic and biogeochemical implications. Precambrian Res 73: 27–49.

Kerans C (1988). Karst-controlled reservoir heterogeneity in Ellenburger Group carbonates of West Texas. AAPG Bull 72: 1160–1183.

Li RX, Wei JY, Yang WD, Guo QJ (2000). Variations of ratio of $^{87}Sr/^{86}Sr$ in seawater with time: implications for sea level changes and global correlation. Adv Earth Sci 15: 729–733 (in Chinese with an abstract in English).

Luo B, Tan XC, Li L, Liu H, Xia JW, Du BQ, Liu XG, Mou XH (2010). Discovery and geologic significance of paleokarst unconformity between Changxing Formation and Feixianguan Formation in Shunan area of Sichuan Basin. Acta Petrol Sin 31: 408–414 (in Chinese with an abstract in English).

Lucia FJ, editor (1999). Carbonate Reservoir Characterization. New York, NY, USA: Springer-Verlag.

Lucia FJ, Kerans C (2003). Carbonate reservoir characterization. J Petrol Tech 55: 70–72.

Ma YS (2008). Geochemical characteristics and origin of nature gases from Puguang Gas Field on Eastern Sichuan Basin. Nat Gas Geosci 19: 1–7 (in Chinese with an abstract in English).

Ma YS, Guo TL, Fu XY (2002). Petroleum geology of marine sequences and exploration potential in Southern China. Mar Origin Petrol Geol 7: 19–27 (in Chinese with an abstract in English).

Ma YS, Guo TL, Zhu GY, Cai XY, Xie ZY (2007a). Simulated experiment evidences of the corrosion and reform actions of H2S to carbonate reservoirs: an example of Feixianguan Formation, East Sichuan. Chin Sci Bull 52: 178–183.

Ma YS, Guo XS, Guo TL, Huang R, Cai XY, Li GX (2007b). Puguang gas field: new giant discovery in the mature Sichuan Basin, Southwest China. AAPG Bull 91: 627–643.

Ma YS, Mou CL, Guo TL, Tan QY, Yu Q (2005). Sequence stratigraphy and reservoir distribution of Feixianguan Formation in Northeastern Sichuan. J Mineral Petrol 25: 73–79 (in Chinese with an abstract in English).

Machel HG, Lonnee J (2002). Hydrothermal dolomite-a product of poor definition and imagination. Sediment Geol 152: 163–171.

Mazzullo SJ (1995). Oil and gas resources in Permian rocks of North America. In: Scholle PA, Peryt TM, Ulmer-Scholle DS, editors. The Permian of Northern Pangea. Berlin, Germany: Springer-Verlag, pp. 259–272.

Mei MX (2010). Stratigraphic impact of the Indo-China Movement and its related evolution of sedimentary-basin pattern of the late Triassic in the middle-upper Yangtze Region, South China. Earth Sci Front 17: 99–111 (in Chinese with an abstract in English).

Mei SL (1995). A new concept for stratigraphic division developed by combining the sequence boundary with the GSSP. Acta Geol Sin 69: 277–284.

Meng QR, Wang E, Hu J (2005). Mesozoic sedimentary evolution of the Northwest Sichuan Basin: implication for continued clockwise rotation of the South China block. Geol Soc Am 117: 396–410.

Meredith DJ, Egan SS (2002). The geological and geodynamic evolution of the Eastern Black Sea Basin: insights from 2-D and 3-D tectonic modeling. Tectonophysics 350: 157–179.

Meyers WJ, Lu FH, Zachariah JK (1997). Dolomitization by mixed evaporative brines and freshwater, upper Miocene carbonates, Nijar, Spain. J Sediment Res 67: 898–912.

No. 2 Sichuan Regional Geological Survey Team of the Sichuan Bureau of Geology, editor (1966). Regional Geological Survey—Nanjiang. Beijing, China: Geological Publishing House (in Chinese).

No. 2 Sichuan Regional Geological Survey Team of the Sichuan Bureau of Geology, editor (1967). Regional Geological Survey—Nanjiang. Beijing, China: Geological Publishing House (in Chinese).

Qiang ZT, editor (2007). Geology of Carbonate Reservoir. Beijing, China: University of Petroleum Press (in Chinese).

Qiao ZF, Li GR, Long SX, Jiang ZZ, Hu WY, Li WM (2010). Characteristics and evolution model of sequence stratigraphy of Feixianguan Formation in the Northeast of Sichuan Basin. Acta Sedimentol Sin 28: 462–470 (in Chinese with an abstract in English).

Ren JS (1984). The Indosinian orogeny and its significance in the tectonic evolution of China. Bull Chin Acad Geo Sci 6: 31–44 (in Chinese with an abstract in English).

Scholle PA, Halley RB (1985). Burial diagenesis: out of sight, out of mind. In: Schneidermann N, Harris PM, editors. Carbonate Cements. Tulsa, OK, USA: SEPM Special Publications, pp. 309–334.

Shen ZY, Xiao AC, Wang L, Guo J, Wei GQ, Zhang L (2010). Unconformity in the lower Triassic of Micangshan area, Northern Sichuan Province: its discovery and significance. Acta Petrol Sin 26: 1313–1321 (in Chinese with an abstract in English).

Tang DQ, Wang LJ, Zeng T, Feng XL (2008). Tectonic evolution function to oil and gas pools reformation in Xuhuan-Daxian area, Northeastern Sichuan Basin. Geosci 22: 230–238 (in Chinese with an abstract in English).

Sichuan Oil & Gas Field Geology Compilation Group, editors (1989). Petroleum Geology of China Sichuan Oil Province, Vol. 10. Beijing, China: Petroleum Industry Press (in Chinese).

Veizer J, Hoefs J (1976). The nature of $^{18}O/^{16}O$ and $^{13}C/^{12}C$ secular trends in sedimentary carbonate rocks. Geochim Cosmochim Ac 40: 1387–1395.

Wang SY, Jiang XQ, Guan HL, Guan YJ (2010). Diagenesis effects of lower Triassic Feixianguan Formation reservoir in Puguang Gas Field, Northeast Sichuan. Petrol Geol Exp 32: 366–372 (in Chinese with an abstract in English).

Wang XZ, Zhang F, Jiang ZB, Zhang JY, Zeng DM (2008). A study of Feixianguan reservoir in Northeast Sichuan Basin. Earth Sci Front 15: 117–122 (in Chinese with an abstract in English).

Wang YG, Liu HY, Wen YC, Yang Y, Zhang J (2002). Distribution law, exploration method and prospectiveness prediction of the oolitic shoal reservoirs in Feixianguan Formation in Northeast Sichuan Basin. Nat Gas Ind 22: 14–19 (in Chinese with an abstract in English).

Wang ZC, Zhao WZ, Peng HY (2002). Characteristics of multi-source petroleum system in Sichuan Basin. Petrol Explor Dev 29: 26–28 (in Chinese with an abstract in English).

Wei GQ, Chen GS, Yang W, Yang Y, Hu MY, Zhang L, Wu SX, Jin H, Shen JH (2004). Sedimentary system of platformal trough of Feixianguan Formation of lower Triassic in Northern Sichuan Basin and its evolution. Acta Sedimentol Sin 22: 254–260 (in Chinese with an abstract in English).

Xia MJ, Deng RJ, Jiang YW, Bi JX, Jin XJ (2010). Determination of the key dissolution stage of oolitic shoal reservoir and discussion of relationship between H2S and anhydrite in Puguang Gas Field. Nat Gas Geosci 21: 68–77 (in Chinese with an abstract in English).

Xu ZQ, Yang JS, Li HQ, Wang RR, Cai ZH (2012). Indosinian collision-orogenic system of Chinese continent and its orogenic mechanism. Acta Petrol Sinica 28: 1697–1709 (in Chinese with an abstract in English).

Yan ZB, Guo FS, Pan JY, Guo GL, Zhang YJ (2005). Application of C, O and Sr isotope composition of carbonates in the research of paleoclimate and paleooceanic environment. Contrib Geol Miner Resour Research 20: 53–56 (in Chinese with an abstract in English).

Yin A, Nie SY (1993). An indentation model for the North and South China collision and the development of the Tan-Lu and Honam Fault systems, Eastern Asia. Tectonics 12: 801–813.

Zhang XT (1958). The nature, stage and distribution range of Indosinian movement and its relationship with guiding the mineral exploration in Southern China. J Bj Inst Geol Expl 3: 31–36 (in Chinese with an abstract in English).

Zhu GY, Zhang SC, Liang YB, Dai JX, Li J (2005a). Isotopic evidence of TSR origin for natural gas bearing high H_2S contents within Feixianguan Formation of the Northeastern Sichuan Basin, Southwestern China. Sci China Ser D Earth Sci 24: 1960–1971.

Zhu GY, Zhang SC, Liang YB, Dai JX, Li J (2005b). Origins of high H2S-bearing natural gas in China. Acta Geol Sin 79: 697–708.